POTSDAM-INSTITUT FÜR KLIMAFOLGENFORSCHUNG

CLIMATE CHANGE

Record Balkan floods of 2014 linked to planetary wave resonance

10.1126/sciadv.1501428

Lisa Stadtherr,[1,2] Dim Coumou,[1]* Vladimir Petoukhov,[1] Stefan Petri,[1] Stefan Rahmstorf[1,3]

In May 2014, the Balkans were hit by a Vb-type cyclone that brought disastrous flooding and severe damage to Bosnia and Herzegovina, Serbia, and Croatia. Vb cyclones migrate from the Mediterranean, where they absorb warm and moist air, to the north, often causing flooding in central/eastern Europe. Extreme rainfall events are increasing on a global scale, and both thermodynamic and dynamical mechanisms play a role. Where thermodynamic aspects are generally well understood, there is large uncertainty associated with current and future changes in dynamics. We study the climatic and meteorological factors that influenced the catastrophic flooding in the Balkans, where we focus on large-scale circulation. We show that the Vb cyclone was unusually stationary, bringing extreme rainfall for several consecutive days, and that this situation was likely linked to a quasi-stationary circumglobal Rossby wave train. We provide evidence that this quasi-stationary wave was amplified by wave resonance. Statistical analysis of daily spring rainfall over the Balkan region reveals significant upward trends over 1950–2014, especially in the high quantiles relevant for flooding events. These changes cannot be explained by simple thermodynamic arguments, and we thus argue that dynamical processes likely played a role in increasing flood risks over the Balkans.

INTRODUCTION

The frequency and intensity of daily precipitation extremes have increased over the last decades in many regions throughout the world (*1*–*4*). On a global scale, this rise can largely be explained by thermodynamic arguments: The increased water-holding capacity of warmer air, as described by the Clausius-Clapeyron equation, intensifies heavy rainfall by about 7% per degree Celsius of warming (*2*, *5*, *6*). These thermodynamic aspects are well understood and reasonably well captured by global climate models, which project further increases in the future, notably over the tropics and high latitudes (*7*, *8*).

Dynamical changes might affect extreme rainfall events in more localized, complex, and nonlinear ways (*9*, *10*). On a local scale, changes in convective regimes as a response to higher temperatures can increase rainfall intensity at a rate exceeding the Clausius-Clapeyron rate (*11*–*14*). In the eastern Mediterranean, sea-surface temperatures have warmed about twice as fast compared to the global oceans (*15*), enhancing the lower tropospheric instability and thereby possibly allowing deep convection to be triggered (*14*). Also, changes in large-scale circulation can affect the occurrence of extreme weather events (*16*–*20*). Several high-impact extreme weather events in the Northern Hemisphere, including heavy rainfall, have been associated with anomalous, high-amplitude, quasi-stationary Rossby waves (*21*, *22*). Recently, wave resonance has been proposed as a common driver behind several of these persistent high-amplitude wave patterns in spring and summer (*21*). Under specific wind conditions, a waveguide can develop in the atmosphere, which reflects planetary waves at northern and southern latitudes, thereby trapping them inside the mid-latitudes and allowing them to resonate. Although this is predicted by theory (*21*), it was also shown statistically in reanalysis data that the presence of resonance conditions is strongly correlated to the presence of high-amplitude, quasi-stationary waves and more extreme surface weather conditions including heavy rainfall (*23*).

One prominent resonance event occurred during the summer of 1997 and was associated with the Great European Flood, which was caused by a Vb cyclone (a particular class of Genoa lows). This class of cyclones tends to originate in the North Atlantic and then head southeast toward the Mediterranean Sea and turn back north toward central and eastern Europe. Carrying warm and moist air from the Mediterranean, they often cause flooding in central and eastern Europe (*24*–*26*). Statistical analysis of Vb cyclones over the period 1971–2000 shows that their accumulated rainfall increases with residence time, which is on average approximately 1 day over central Europe (8°E to 22°E/48°N to 51°N) (*27*). Only one detected Vb cyclone had a residence time exceeding 2.5 days: During the summer of 1997, cyclone "Zoe" persisted over central Europe for 4.5 days, leading to massive flooding (*27*).

The hemispheric flow during that summer fulfilled resonance conditions, likely magnifying the observed high-amplitude, quasi-stationary circumglobal planetary wave (*21*). This wave was characterized by a persistent pattern of southward flow over western Europe and northward flow over central Europe, forming the right background flow for a typical Vb cyclone track. Recent years have seen a cluster of such resonance events in the Northern Hemisphere (*23*). Generally, climate models struggle in capturing summertime Rossby waves and blockings (*9*, *17*), and likewise, there is large uncertainty in future projections of circulation-related fields (*28*, *29*). An improved understanding of the underlying dynamical mechanisms is thus critical.

RESULTS

Balkan floods of May 2014

Here, we examine the climatic and meteorological factors that led to the disastrous flooding in the Balkans in May 2014. In the main affected region, the Sava River basin in Bosnia and Herzegovina, the

[1]Potsdam Institute for Climate Impact Research, Earth System Analysis, 14473 Potsdam, Germany. [2]Christian-Albrechts-Universität zu Kiel, 24118 Kiel, Germany. [3]University of Potsdam, 14469 Potsdam, Germany.
*Corresponding author. E-mail: coumou@pik-potsdam.de

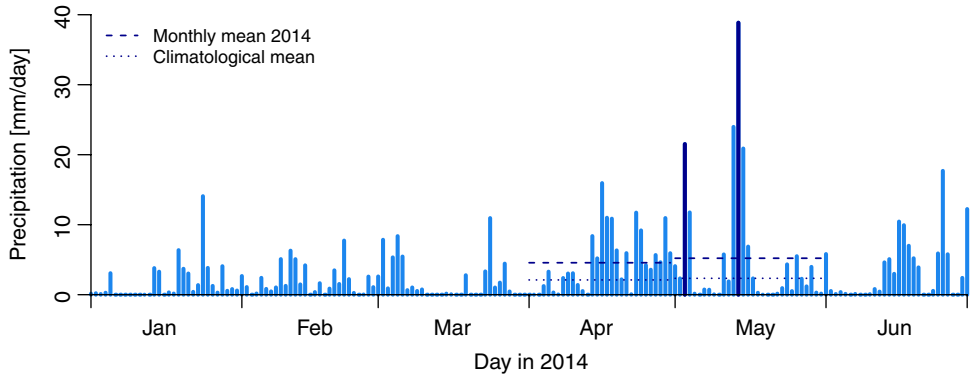

Fig. 1. Daily precipitation averaged over the BHSC region during the first half of 2014, showing clusters of heavy rainfall in April and around 3 May (dark blue), before the record-breaking rainfall events associated with cyclone Yvette (14 May; dark blue). Horizontal lines indicate monthly means for April and May 2014 (dashed) and their climatology (dotted).

rainfall between 14 and 19 May 2014 set record values in the 120-year observational data (*30*). The economic damage was estimated at up to €3.5 billion for Serbia and Bosnia and Herzegovina, and several dozen casualties were reported (*31*). Unusually, rainy conditions in April and early May provided a favorable precondition for the flooding event in the Balkans in mid-May 2014. Figure 1 provides daily rainfall averaged over Bosnia and Herzegovina, Serbia, and Croatia (hereafter the BHSC region) during the first half of 2014, showing several clusters of heavy rain in late April and early May. On 3 and 4 May, nearly 50% of the May 1950–2013 climatological precipitation (of ~70 mm/month) fell in only 48 hours. The maximum 2-day precipitation reached 61.6 mm locally, amounting to 85% of the May climatology. These sustained wet conditions over several weeks strongly increased soil moisture content and thus were an important factor for the later flooding event (see figs. S1 and S2).

On 13 May, the cyclone (internationally named "Yvette") moved over the Mediterranean Sea heading to southeastern Europe. Supplied with moist and warm air from the Adriatic Sea, it reached the Balkan Peninsula, where the air experienced strong orographic lifting over the Dinaric Alps. This led to extraordinary high precipitation amounts, which were sustained over 4 days. Only by 17 May did the cyclone leave the Balkan region, moving northward to Poland.

The rainfall amounts from this cyclone far surpassed the values of the previous weeks. The 4-day rainfall (13 to 16 May), shown in Fig. 2, exceeded 90 mm on average in the BHSC region, which is substantially more than the May climatology. Most rain fell on 14 May, with the region receiving nearly 40 mm (see Fig. 1). The maximum amount accumulated over these 4 days reached 210.5 mm in a location roughly at the border between Serbia and Bosnia, corresponding to almost three times the climatological precipitation in May in that area (Fig. 2). The highest daily rainfall rate exceeded 100 mm in the same region on 14 May, setting a new record in the observational period (fig. S1).

Figure 2 shows the cyclone track based on the lowest core pressures and provides evidence for the near stationarity of the cyclone during the flooding event. For at least 72 hours (from 13 May 6:00 a.m. to 16 May 6:00 a.m.), the cyclone's core was in close proximity to the BHSC region, before moving further northward on the typical Vb storm track. This track closely matches the patterns of the 4-day rainfall analysis, with the highest precipitation amounts observed on 13 to 15 May 2014 (fig. S1).

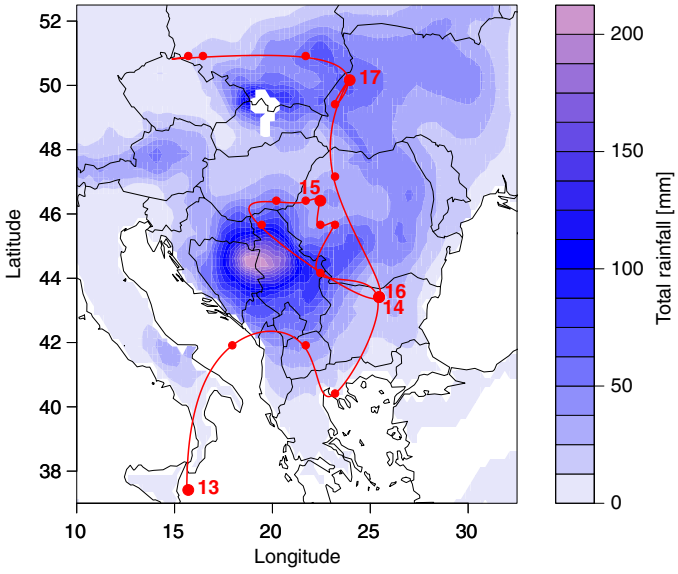

Fig. 2. Accumulated rainfall (blue colors) over southeastern Europe from 13 to 16 May 2014 (in millimeters) and the position of cyclone Yvette tracked by its lowest core pressures (red line). Large red dots represent the position at 12:00 a.m. with the date labeled, and small red dots indicate positions at 6:00 a.m., 12:00 p.m., and 6:00 p.m.

Quantile regressions

To quantify how unusual such rainfall amounts are, we performed quantile regressions of daily precipitation over the BHSC region during spring (March, April, May, and June; hereafter MAMJ) over the 1950–2014 period (Fig. 3). A significant upward trend is detected in the mean daily rainfall, although the magnitude of change is small (~0.005 mm/day per year). Much more pronounced upward trends are detected in the upper quantiles between 90 and 99%, that is, those relevant for flooding events. The 99th percentile (with a value of about 14 mm/day) in particular shows a strong upward trend of about 5 mm/day over 65 years (0.07 mm/day per year, that is, more than 10 times larger than the mean trend), reflecting an increase in rainfall intensity of about 35%. Regional

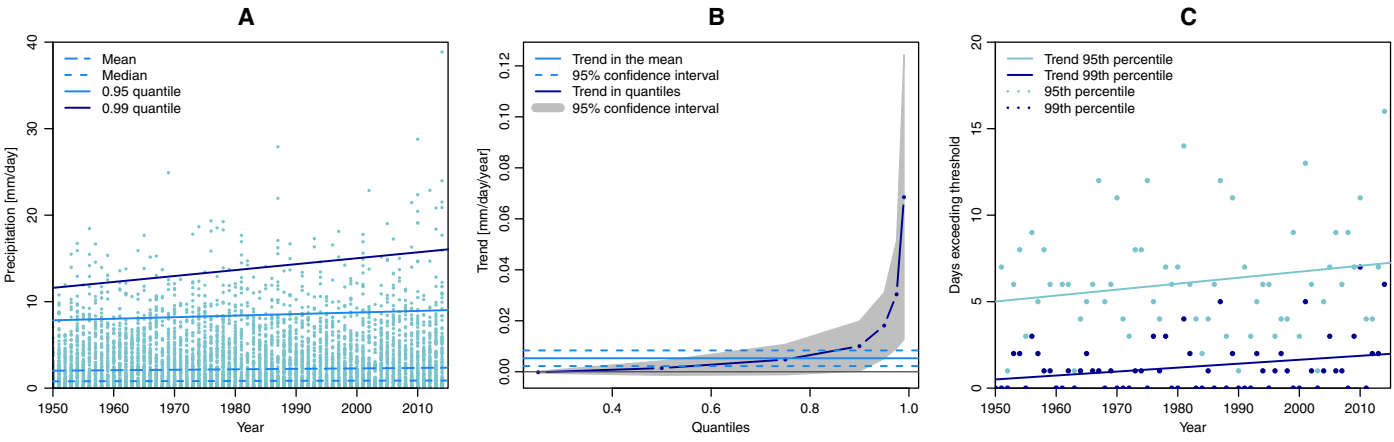

Fig. 3. Increased heavy rainfall days over the BHSC region during spring. (**A**) Daily rainfall distribution for days in MAMJ (dots) plus linear regressions of the mean, median, and the 95th and 99th quantile for 1950–2014. (**B**) Linear trend of different quantiles in daily rainfall during spring showing strong and significant trends in the upper tail. (**C**) Number of days exceeding the 95th and 99th rainfall percentile during spring in the BHSC region.

spring temperatures warmed by ~1°C over 1950–2014 (fig. S3) and thus the increased water-holding capacity can only explain an increase in rainfall intensity of 1 mm/day over this period (7% of 14 mm/day). Thermodynamics can only explain a fraction of the observed increase in rainfall intensity of 5 mm/day. Upper quantile trends have broader confidence intervals, compared to the median, as fewer data are available, but are nevertheless highly significant (Fig. 3B). This has increased the probability of extreme rainfall events, with the number of days exceeding the 99th percentile more than doubling (see Fig. 3C).

Hemispheric wind field analysis

To understand the near stationarity of cyclone Yvette, we analyzed the hemispheric scale circulation patterns during May 2014. The wind field at 300 hPa on 13 May (Fig. 4A) shows strongly meandering jet stream patterns in the Northern Hemisphere mid-latitudes. These meandering patterns were due to a strong contribution of a quasi-stationary wave with wave number $k = 6$, as can be seen in the roughly six peaks of the meridional wind component (v) at relatively regular distances in the 15-day running mean data (see Fig. 4B). Spectral analyses confirm that wave 6 was indeed the dominant contributor to the large-scale flow (Fig. 4C). The large v amplitudes in the 15-day running mean data, up to 20 m/s locally (usual values are around 5 m/s), indicate that this wave is indeed quasi-stationary (from 6 to 20 May 2014). This wave pattern was characterized by a persistent southward flow over western Europe (blue region stretching from Netherlands to southern Italy) and a persistent northward flow over eastern Europe (red region north of the Black Sea), as can also be seen in the total wind field (Fig. 4A). Thus, these analyses indicate that the typical Vb cyclone track and unusual near-stationary weather situation were facilitated by a quasi-stationary Rossby wave.

During the period immediately before and after the flooding event, the pattern of the zonal mean zonal wind (U) satisfied the conditions for wave resonance in the upper level flow (*21*). The main condition for resonance is the formation of a zonally directed waveguide, which depends on the shape of U and on the wave number k of the trapped wave only. As derived from the barotropic vorticity equation on a sphere and discussed by Petoukhov *et al.* (*21*), the square of the meridional wave number (l^2) is given by

$$l^2(U,k,\varphi) = \frac{2\Omega\cos^3\varphi}{aU} - \frac{\cos^2\varphi}{a^2U}\frac{d^2U}{d\varphi^2} + \frac{\sin\varphi\cos\varphi}{a^2U}\frac{dU}{d\varphi} + \frac{1}{a^2} - \left(\frac{k}{a}\right)^2$$

where a is Earth's radius, Ω is its angular velocity, φ is latitude, and l is a complex number. For a waveguide to form, l^2 has to be positive inside the waveguide and has to change sign at its latitudinal boundaries, or turning points, such that the wave's energy is largely reflected. Waves of this particular wave number k thus become a preferred mode of oscillation of the atmosphere. If this preferred value of k is an integer (or at least close to one), a quasi-stationary wave circling the whole globe in the mid-latitudes is set up, which may resonate with the thermal and orographic forcing pattern and thus grow to large amplitude. In contrast, waves with values of k for which no waveguide exists can disperse out of the mid-latitudes toward the pole and the equator and therefore decay rapidly.

To check for the presence of a waveguide, we plot ($l^2a^2 + k^2$) for the 15-day running mean data centered on 13 May 2014 (Fig. 4D), which thus solely depends on U and latitude (as seen by multiplying the equation by a^2 and moving the last term to the left side). The right vertical axis gives the corresponding k values for $l^2 = 0$, that is, for the turning points. Two turning points at sufficiently large distance emerge for $k = 6$ at 34°N and 40°N, with positive values of l^2 (a "hump") in between. Thus, a waveguide for wave $k = 6$ exists (that is, straight resonance, as k is an integer number; see the Supplementary Materials), effectively trapping it in the mid-latitudes, and its quasi-stationary component can therefore be amplified by resonance with thermal and orographic forcing.

The second major condition for resonant growth of planetary wave amplitudes is the presence of a matching forcing, in this case at wave number 6. Equation 3 in Petoukhov *et al.* (*21*) predicts the amplitude of resonant waves from the amplitude of the forcing at the resonant wave

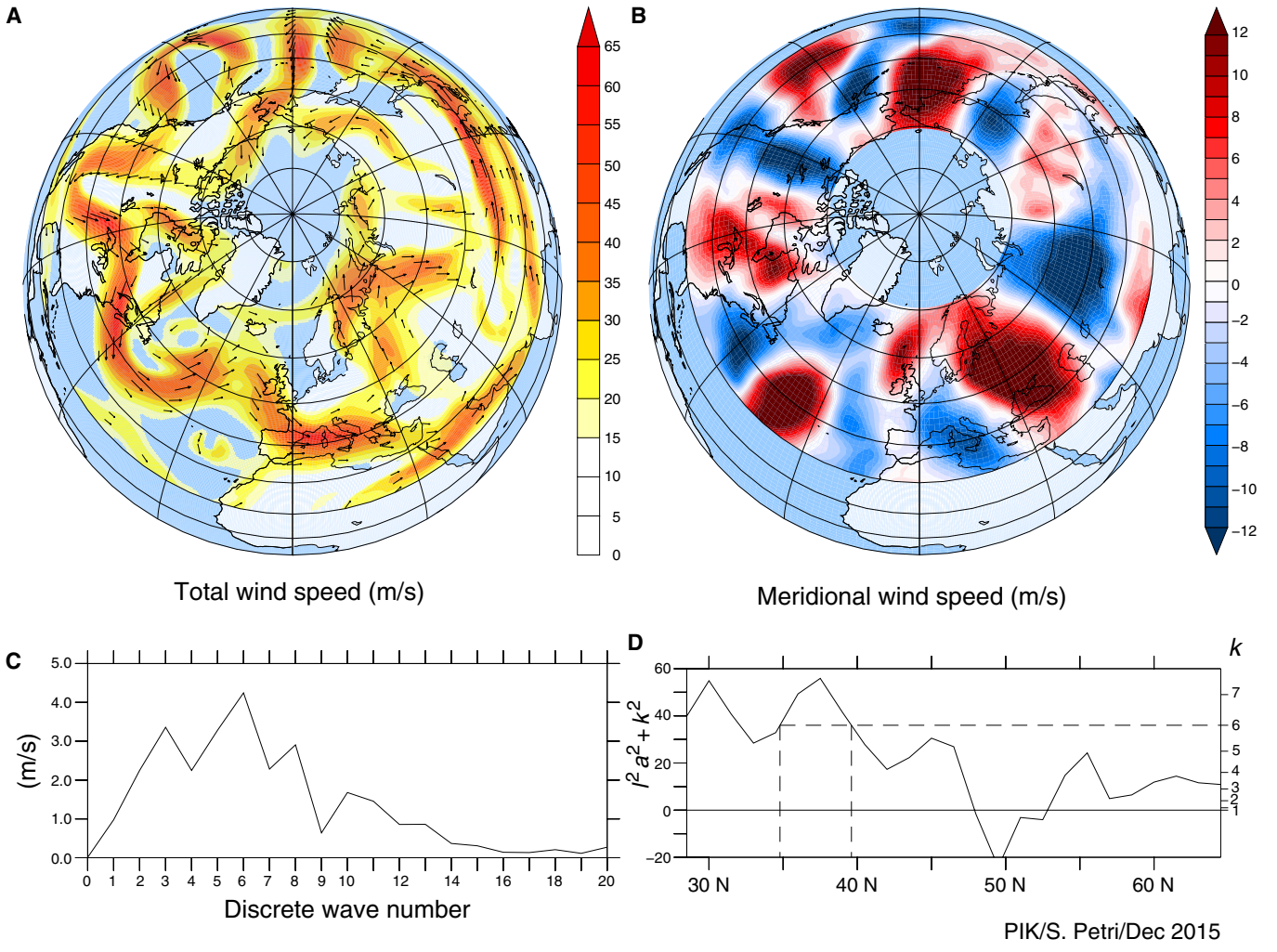

Fig. 4. Upper-level hemispheric circulation in May 2014. (**A**) Total wind field (in meters per second) at 300 mb over the Northern Hemisphere midlatitudes on 13 May (daily mean). Color displays the magnitude of the flow, and arrows indicate direction. (**B**) Meridional component of the wind speed (in meters per second) averaged from 6 to 20 May 2014, revealing a quasi-stationary wave 6 pattern. (**C**) Spectral contributions of different wave numbers to the meridional wind field averaged from 35°N to 60°N and from 6 to 20 May 2014. (**D**) Latitudinal distribution of the square of the stationary wave number given by $(l^2a^2 + k^2)$, which gives the location of possible turning points for any given k indicated on the right vertical axis. It shows that a waveguide for wave number 6 forms from 34°N to 40°N (dashed lines). The vertical dashed black lines indicate the latitudinal positions of the turning points for wave number 6 as given by the crossing of the horizontal dashed black lines with the right y axis.

number, including the effect of atmospheric friction, which limits the final amplitude. The amplitude of orographic and thermal forcing is calculated from the topography data and the temperature fields in the reanalysis data. The resulting predicted amplitude of the resonant wave 6 during the Balkan flooding event is 3.4 to 7.6 m/s, with the uncertainty stemming from the estimated magnitude of the friction term (see the Supplementary Materials). This predicted amplitude of the resonant wave matches the observed amplitude of ~4 m/s of the quasi-stationary wave 6.

DISCUSSION

The reported co-occurrence of resonance and a quasi-stationary Vb cyclone in May 2014 does not demonstrate a direct link between the two phenomena. Still, the two most persistent Vb cyclones in the reanalysis data occurred during resonance conditions, that is, cyclone Zoe in 1997 and cyclone Yvette in 2014, both causing massive flooding. In a wider sense, the statistical relationship between resonance, slow wave speeds, and surface extremes, including heavy rainfall, has been demonstrated in data (*23*), as also predicted by theory (*21*). Therefore, we conclude that the quasi-stationarity of cyclone Yvette and, therefore, the flooding event itself were made more likely due to the presence of resonance conditions. A statistical quantification of the relationship between resonance and quasi-stationary Vb cyclones is hampered by the shortness of the time series and the rareness of both phenomena.

This study has identified several factors that contributed to the extreme flooding in the Balkans in spring 2014. First of all, the flooding was caused by heavy rain falling over a period of 4 days on already wet

soils. The precipitation amounts connected to the low-pressure system Yvette exceeded record values and were initiated by orographic lifting of the cyclone on the Vb storm track. Further, we show that during the days of flooding, the cyclone was almost stationary over the Balkan region. This weather situation was linked to a high-amplitude, quasi-stationary Rossby wave likely amplified by hemispheric wave resonance. We thus present evidence that the extreme flooding event in the BHSC region was related to a strong wave 6 flow pattern under resonance conditions. Upward trends in the heaviest rainfall, as shown with quantile regressions, greatly exceed the 7% per degree Celsius of warming expected from the Clausius-Clapeyron equation. Thus, simple warming cannot explain the magnitude of the trend, indicating that changes in dynamical processes, due to either natural variability or anthropogenic climate change, are important.

Our findings are in agreement with the recent cluster of resonance events leading to high-amplitude, quasi-stationary waves (*23*). Resonance conditions have been found to be fulfilled for many recent weather extremes, which caused devastation especially due to their persistence. Substantial changes have been detected in the Northern Hemisphere warm season circulation over the last decades: The zonal mean flow and storm tracks have weakened (*32*, *33*), and the frequency and persistence of blocking anticyclones appear to have increased in summer over several mid-latitude regions, including Europe and western Asia (*34*). These dynamical changes indicate more persistent warm season circulation in the mid-latitudes, especially over Europe and western Asia, and are thus favorable for the occurrence of the synoptic situation analyzed here. Moreover, our study highlights the importance of resonant circulation regimes in steering Vb cyclones and, thereby, in triggering extreme flooding in central and eastern Europe. In future work, we will aim to understand the underlying drivers of resonance events and to quantify their effect on weather patterns in different Northern Hemisphere regions.

METHODS

Observations

To estimate the precipitation amounts in the affected area, daily observational precipitation totals were extracted from the European Climate Assessment and Dataset using the E-OBS daily gridded data set (*35*). This set was used because of the regular 0.25° × 0.25° high-resolution grid and the relatively long time series starting from 1950 to June 2014. It contains land-only data covering the European region in 25°N to 75°N longitude and 40°W to 75°E latitude.

Reanalysis

To detect and track the cyclone, we used sea level pressures from ERA-Interim reanalysis (*36*). These 6-hourly data come at a high spatial resolution of 0.75° × 0.75° on a global Gaussian grid. To estimate the saturation of the soils, we used daily values for volumetric soil water layer of four different layers between depths of 0 and 255 cm below land surface. We also analyzed daily mean zonal (U) and meridional (v) wind components at different pressure levels.

Land mask

To extract the area-averaged values and cumulative precipitation in the affected region, we created a land mask. Therefore, grid information about latitudes and longitudes of the BHSC region was extracted from the database of global administrative areas. This way, a mask is constructed with the same resolution as the E-OBS precipitation grid (0.25° × 0.25°). Using this land mask, area-averaged precipitation anomalies for the period January to June 2014 were computed with respect to the 1950–2013 climatology.

Quantile regressions

Trend analyses were made for the daily precipitation totals over the full time period of 65 years. The statistical significance was determined using quantile regression. Trend analyses can be made with a diversity of techniques. Here, the method of ordinary least squares for linear regression was used in addition to the quantile regression, where the median served as a solution for the minimization problem of the sum of absolute residuals. This method can be applied for each quantile of the distribution function separately, and therefore, it is more robust in handling outliers and applicable to asymmetrical distributions (*37*).

Cyclone track

To reproduce the pathway of this individual cyclone, 6-hourly sea level pressure fields from ERA-Interim were used (*36*).

SUPPLEMENTARY MATERIALS

Supplementary material for this article is available at http://advances.sciencemag.org/cgi/content/full/2/4/e1501428/DC1

Amplitude calculation

fig. S1. Daily precipitation totals (in millimeters) for several days of May 2014.

fig. S2. Anomalies for mean volumetric soil water layers (soil moisture) in April and May 2014.

fig. S3. Spring (MAMJ) Goddard Institute for Space Studies surface temperature anomalies over the region extending from 12°E to 28°E and from 32°N to 46°N showing that warming in this region has been about 1°C since 1950.

References (*38*–*40*)

REFERENCES AND NOTES

1. S. Westra, L. V. Alexander F. W. Zwiers, Global increasing trends in annual maximum daily precipitation. *J. Climate* **26**, 3904–3918 (2013).
2. J. Lehmann, D. Coumou, K. Frieler, Increased record-breaking precipitation events under global warming. *Clim. Change* **132**, 501–515 (2015).
3. P. Y. Groisman, R. W. Knight, D. R. Easterling, T. R. Karl, G. C. Heger, V. N. Razuvaev, Trends in intense precipitation in the climate record. *J. Climate* **18**, 1326–1350 (2005).
4. N. Nicholls, S. Seneviratne, Chapter 3: Changes in climate extremes and their impacts on the natural physical environment, in *Managing the Risks of Extreme Events and Disasters to Advance Climate Change Adaptation,* M. Rusticucci, V. Semenov, Eds. (Cambridge Univ. Press, Cambridge, 2012).
5. S.-K. Min, X. Zhang, F. W. Zwiers, G. C. Hegerl, Human contribution to more-intense precipitation extremes. *Nature* **470**, 378–381 (2011).
6. X. Zhang, H. Wan, F. W. Zwiers, G. C. Hegerl, S.-K. Min, Attributing intensification of precipitation extremes to human influence. *Geophys. Res. Lett.* **40**, 5252–5257 (2013).
7. K. E. Trenberth, Changes in precipitation with climate change. *Clim. Res.* **47**, 123–138 (2011).
8. J. Sillmann, V. V. Kharin, F. W. Zwiers, X. Zhang, D. Bronaugh, Climate extremes indices in the CMIP5 multi-model ensemble. Part 2: Future climate projections. *J. Climate* **118**, 2473–2493 (2013).
9. K. E. Trenberth, J. T. Fasullo, T. G. Shepherd, Attribution of climate extreme events. *Nat. Clim. Change* **5**, 725–730 (2015).
10. D. Coumou, S. Rahmstorf, A decade of weather extremes. *Nat. Clim. Change* **2**, 491–496 (2012).
11. G. Lenderink, E. van Meijgaard, Increase in hourly precipitation extremes beyond expectations from temperature changes. *Nat. Geosci.* **1**, 511–514 (2008).
12. J. O. Haerter, P. Berg, Unexpected rise in extreme precipitation caused by a shift in rain type? *Nat. Geosci.* **2**, 372–373 (2009).
13. P. Berg, C. Moseley, J. O. Haerter, Strong increase in convective precipitation in response to higher temperatures. *Nat. Geosci.* **6**, 181–185 (2013).

14. E. P. Meredith, V. A. Semenov, D. Maraun, W. Park, A. V. Chernokulsky, Crucial role of Black Sea warming in amplifying the 2012 Krymsk precipitation extreme. *Nat. Geosci.* **8**, 615–619 (2015).
15. Y. Samuel-Rhoads, G. Zodiatis, A. Nikolaidis, D. Hayes, G. Georgiou, G. Konnaris, M. Nikolaides, Climate change impacts on sea surface temperature in the eastern Mediterranean, Levantine basin. *Proc. SPIE* **8795**, 87950N (2013).
16. G. Branstator, Circumglobal teleconnections, the jet stream waveguide, and the North Atlantic oscillation. *J. Climate* **15**, 1893–1910 (2002).
17. S. Schubert, H. Wang, M. Suarez, Warm season subseasonal variability and climate extremes in the Northern Hemisphere: The role of stationary Rossby waves. *J. Climate* **24**, 4773–4792 (2011).
18. Y. Tachibana, T. Nakamura, H. Komiya, M. Takahashi, Abrupt evolution of the summer Northern Hemisphere annular mode and its association with blocking. *J. Geophys. Res.* **115**, 13 (2010).
19. K. E. Trenberth, J. T. Fasullo, Climate extremes and climate change: The Russian heat wave and other climate extremes of 2010. *J. Geophys. Res. Atmos.* **117**, D17103 (2012).
20. W. K. M. Lau, K.-M. Kim, The 2010 Pakistan flood and Russian heat wave: Teleconnection of hydrometeorological extremes. *J. Hydrometeorol.* **13**, 392–403 (2012).
21. V. Petoukhov, S. Rahmstorf, S. Petri, H. J. Schellnhuber, Quasiresonant amplification of planetary waves and recent Northern Hemisphere weather extremes. *Proc. Natl. Acad. Sci. U.S.A.* **110**, 5336–5341 (2013).
22. J. A. Screen, I. Simmonds, Amplified mid-latitude planetary waves favour particular regional weather extremes. *Nat. Clim. Change* **4**, 704–709 (2014).
23. D. Coumou, V. Petoukhov, S. Rahmstorf, S. Petri, H. J. Schellnhuber, Quasi-resonant circulation regimes and hemispheric synchronization of extreme weather in boreal summer. *Proc. Natl. Acad. Sci. U.S.A.* **111**, 12331–12336 (2014).
24. M. Mudelsee, M. Börngen, G. Tetzlaff, U. Grünewald, Extreme floods in central Europe over the past 500 years: Role of cyclone pathway "Zugstrasse Vb". *J. Geophys. Res. Atmos.* **109**, D23101 (2004).
25. Z. W. Kundzewicz, U. Ulbrich, T. Brücher, D. Graczyk, A. Krüger, G. C. Leckebusch, L. Menzel, I. Pínskwar, M. Radziejewski, M. Szwed, Summer floods in Central Europe—Climate change track? *Nat. Hazards* **36**, 165–189 (2005).
26. W. J. Van Bebber, *Die Wettervorhersage* (Enke, Stuttgart, 1898).
27. K. M. Nissen, U. Ulbrich, G. C. Leckebusch, Vb cyclones and associated rainfall extremes over Central Europe under present day and climate change conditions. *Meteorol. Z.* **22**, 649–660 (2013).
28. T. G. Shepherd, Atmospheric circulation as a source of uncertainty in climate change projections. *Nat. Geosci.* **7**, 703–708 (2014).
29. S. Bony, B. Stevens, D. M. W. Frierson, C. Jakob, M. Kageyama, R. Pincus, T. G. Shepherd, S. C. Sherwood, A. P. Siebesma, A. H. Sobel, M. Watanabe, M. J. Webb, Clouds, circulation and climate sensitivity. *Nat. Geosci.* **8**, 261–268 (2015).
30. G. J. Van Oldenborgh, Climate aspects of the floods in Bosnia and Serbia May 2014 (2014); www.knmi.nl/cms/content/119609/climate_aspects_of_the_floods_in_bosnia_and_serbia_may_2014.
31. L. Gaál, R. Beranová, K. Hlavčová, J. Kyselý, Climate change scenarios of precipitation extremes in the carpathian region based on an ensemble of regional climate models. *Adv. Meteorol.* **2014**, 1–14 (2014).
32. D. Coumou, J. Lehmann, J. Beckmann, The weakening summer circulation in the Northern Hemisphere mid-latitudes. *Science* **348**, 324–327 (2015).
33. J. Lehmann, D. Coumou, The influence of mid-latitude storm tracks on hot, cold, dry, and wet extremes. *Sci. Rep.* **5**, 1–9 (2015).
34. D. E. Horton, N. C. Johnson, D. Singh, D. L. Swain, B. Rajaratnam, N. S. Diffenbaugh, Contribution of changes in atmospheric circulation patterns to extreme temperature trends. *Nature* **522**, 465–469 (2015).
35. M. R. Haylock, N. Hofstra, A. M. G. K. Tank, E. J. Klok, P. D. Jones, M. New, A European daily high-resolution gridded data set of surface temperature and precipitation for 1950–2006. *J. Geophys. Res. Atmos.* **113**, D20119 (2008).
36. D. P. Dee, S. M. Uppala, A. J. Simmons, P. Berrisford, P. Poli, S. Kobayashi, U. Andrae, M. A. Balmaseda, G. Balsamo, P. Bauer, P. Bechtold, A. C. M. Beljaars, L. van de Berg, J. Bidlot, N. Bormann, C. Delsol, R. Dragani, M. Fuentes, A. J. Geer, L. Haimberger, S. B. Healy, H. Hersbach, E. V. Hólm, L. Isaksen, P. Kållberg, M. Köhler, M. Matricardi, A. P. McNally, B. M. Monge-Sanz, J.-J. Morcrette, B.-K. Park, C. Peubey, P. de Rosnay, C. Tavolato, J.-N. Thépaut, F. Vitart, The ERA-Interim reanalysis: Configuration and performance of the data assimilation system. *Q. J. Roy. Meteorol. Soc.* **137**, 553–597 (2011).
37. R. Koenker, K. F. Hallock, Quantile Regression. *J. Econ. Perspect.* **15**, 143–156 (2001).
38. D. A. Hastings, P. K. Dunbar, *Global Land One-Kilometer Base Elevation (GLOBE)* (1999).
39. E. Kalnay, M. Kanamitsu, R. Kistler, W. Collins, D. Deaven, L. Gandin, M. Iredell, S. Saha, G. White, J. Woollen, Y. Zhu, A. Leetmaa, R. Reynolds, The NCEP/NCAR 40-year reanalysis project. *B. Am. Meteorol. Soc.* 437–471 (1996).
40. J. G. Charney, A. Eliassen, A numerical method for predicting the perturbations of the middle latitude westerlies. *Tellus* **1**, 39–54 (1949).

Acknowledgments: Comments by two anonymous reviewers have considerably improved the manuscript. **Funding:** This work was supported by the German Federal Ministry of Education and Research (01LN1304A). The publication of this article was funded by the Open Access Fund of the Leibniz Association. **Author contributions:** L.S. and S.P. performed analysis. All authors contributed to the design of the research and to the writing of the manuscript. **Competing interests:** The authors declare that they have no competing interests. **Data and materials availability:** All data needed to evaluate the conclusions in the paper are presented in the paper and/or the Supplementary Materials. Additional data related to this paper may be requested from the authors. Data presented in this manuscript will be archived for at least 10 years by the Potsdam Institute for Climate Impact Research.

Submitted 12 October 2015
Accepted 24 March 2016
Published 15 April 2016
10.1126/sciadv.1501428

Citation: L. Stadtherr, D. Coumou, V. Petoukhov, S. Petri, S. Rahmstorf, Record Balkan floods of 2014 linked to planetary wave resonance. *Sci. Adv.* **2**, e1501428 (2016).

ScienceAdvances
AAAS

Record Balkan floods of 2014 linked to planetary wave resonance

Lisa Stadtherr, Dim Coumou, Vladimir Petoukhov, Stefan Petri and Stefan Rahmstorf (April 15, 2016)
Sci Adv 2016, 2:.
doi: 10.1126/sciadv.1501428